

Closed-Loop Fuzzy Energy Regulation in Patients with Hypercortisolism via Inhibitory and Excitatory Intermittent Actuation

Hamid Fekri Azgomi ¹, Jin-Oh Hahn ², and Rose T. Faghah ^{1,*}

¹ Computational Medicine Lab, Department of Electrical and Computer Engineering, University of Houston, Houston, TX, USA

² Department of Mechanical Engineering, University of Maryland, College Park, MD, USA

Correspondence*:
Rose T. Faghah
rtfaghah@uh.edu

2 ABSTRACT

3 Hypercortisolism or Cushing's disease, which corresponds to the excessive levels of cortisol
4 hormone, is associated with tiredness and fatigue during the day and disturbed sleep at night. Our
5 goal is to employ a wearable brain machine interface architecture to regulate one's energy levels in
6 hypercortisolism. In the present simulation study, we generate multi-day cortisol profile data for ten
7 subjects both in healthy and disease conditions. To relate an internal hidden cognitive energy state
8 to one's cortisol secretion patterns, we employ a state-space model. Particularly, we consider
9 circadian upper and lower bound envelopes on cortisol levels, and timings of hypothalamic
10 pulsatile activity underlying cortisol secretions as continuous and binary observations, respectively.
11 To estimate the hidden cognitive energy-related state, we use Bayesian filtering. In our proposed
12 architecture, we infer one's cognitive energy-related state using wearable devices rather than
13 monitoring the brain activity directly and close the loop utilizing fuzzy control. To model actuation
14 in the real-time closed-loop architecture, we simulate two types of medications that result in
15 increasing and decreasing the energy levels in the body. Finally, we close the loop using a
16 knowledge-based control approach. The results on ten simulated profiles verify how the proposed
17 architecture is able to track the energy state and regulate it using hypothetical medications. In a
18 simulation study based on experimental data, we illustrate the feasibility of designing a wearable
19 brain machine interface architecture for energy regulation in hypercortisolism. This simulation
20 study is a first step towards the ultimate goal of managing hypercortisolism in real-world situations.

21 **Keywords:** Closed-Loop, Energy State, Cortisol, Hypercortisolism, Bayesian Estimation, Wearable, Fuzzy Control, Cushing's

1 INTRODUCTION

22 The cortisol hormone is the main stress hormone in an individual's body which is secreted in a pulsatile
23 process (Azgomi and Faghah, 2019; Smyth et al., 2020; Wickramasuriya and Faghah, 2019b; Taghvafard
24 et al., 2019). Cortisol secretion patterns, which are mainly controlled by the hypothalamus, are critical in
25 assessing various functionalities such as regulating blood pressure and adjusting blood glucose levels. So,
26 investigating changes in cortisol secretion would shed some light on one's internal energy state variations
27 (Smyth et al., 2020; Wickramasuriya and Faghah, 2019b; Faghah, 2018). Adrenocorticotropic hormone

28 (ACTH) (i.e. a tropic hormone) causes the adrenal cortex to release cortisol in a pulsatile manner (Hakamata
29 et al., 2017; Pednekar et al., 2020, 2019). The hypothalamus employs corticotrophin-releasing hormone
30 (CRH) to stimulate the anterior pituitary to produce ACTH (Faghah et al., 2014; Faghah, 2014). Any
31 irregular patterns in cortisol secretions (e.g. too much cortisol release, which is called hypercortisolism, or
32 not providing a sufficient amount of cortisol, which is called hypocortisolism) may cause the imbalance in
33 internal energy variations (Harris et al., 2015; Arnold, 2008; D'Angelo et al., 2015). These irregularities,
34 which are common among the Cushing's patients who are exposed to the hypercortisolism, lead them to
35 feel fatigue during the daytime and sleep problems at night (Vance, 2017; Stalder et al., 2016). Insufficient
36 release of cortisol early in the morning may result in feeling fatigue during the day. On the other hand, high
37 levels of cortisol in the evening might cause sleep disturbances at night (Dwyer et al., 2019).

38 While the initial treatment option for Cushing's disease is a surgery with a 78% success rate, evidence
39 shows that the relapse happens in almost 13% of patients (Driessens et al., 2018). For the patients in whom
40 the surgery is not successful or feasible, medical therapy is unavoidable (Pivonello et al., 2015). Due to
41 recent advances in employing novel compounds that can regulate cortisol secretions, medical therapy
42 has attracted more attention (Tritos and Biller, 2017). Nowadays, medical therapy is being suggested in
43 different ways: pre-surgical treatment, post-surgical options for the patients that fail the surgical option, and
44 the primary remedy for those in whom the surgery is not considered as an option (Pivonello et al., 2015).

45 The clinical observations in Cushing's syndrome patients clearly demonstrate a role for the HPA axis in
46 the regulation of energy balance (Nieuwenhuizen and Rutters, 2008; Björntorp and Rosmond, 2000;
47 Wickramasuriya and Faghah, 2019b). While there exist multiple factors to understand one's energy
48 variations, there is not any specific method to directly infer internal energy state. Hence, it is not possible
49 to present the evidence to show the correlation between energy state and cortisol variations. However, there
50 is evidence that patients with irregular cortisol patterns experience fatigue during day time and disturbed
51 sleep cycles at night. For example, authors in (Pednekar et al., 2019, 2020) have shown that the patients
52 with fibromyalgia syndrome, which is also associated with the irregular patterns in cortisol secretions,
53 experience fatigue during the day and sleep disorders at night. Researchers in (Crofford et al., 2004)
54 identified lower cortisol levels in the patients with chronic fatigue syndrome. This evidence verifies the
55 potential correlation between cortisol measurements and internal energy state.

56 As it is discussed, patients with Cushing's syndrome have disturbed circadian rhythm in their sleep cycles.
57 In this regard, medications with inhibitory effects to lower the energy state and help the subjects with more
58 balanced sleep cycles could be helpful. An example of these types of medications could be Melatonin. In
59 the literature, it has been indicated that excessive cortisol secretions associated with Cushing's disease may
60 lead to an irregular Melatonin rhythm (Zisapel et al., 2005; James et al., 2007). So, taking the advantages of
61 Melatonin in improving sleep cycles, we can suggest using this medication for inhibitory effects. Although
62 patients with hypercortisolism usually experience high levels of energy during the evening, they may suffer
63 a lack of sufficient energy levels during the daytime (Pednekar et al., 2020, 2019). As a result, the need for
64 medications to elevate the energy levels is unavoidable. Medications with excitatory effects to enhance
65 energy state and prevent the subjects to feel fatigue during the daytime would be helpful in this regard.
66 An example of these types of medications could be Methylphenidate. As patients with hypercortisolism
67 suffer from not having enough energy levels in the daytime, medications like Methylphenidate could be
68 suggested while implementing the proposed approach in the real world. In literature, it has been validated
69 that taking two doses of Methylphenidate is significantly effective in relieving fatigue (Blockmans et al.,
70 2006; Chaudhuri and Behan, 2004).

71 Due to the potential medications' side-effects, tolerance, and resistance that a person shows against the
72 use of specific medications, it is highly important to establish a supervision layer that enables automated
73 regulation of medication usage (Fleseriu et al., 2019). We propose our approach by taking the advantages of
74 wearable-type devices capable of monitoring blood cortisol in a non-invasive way as a feedback modality
75 for such supervision. The proposed approach is the first attempt to automate the regulation of medications
76 required to manage the energy levels in patients with hypercortisolism in a closed-loop manner (Figure 1).

77 Recently, there has been an increased interest in employing control theory in advancing modern
78 medication therapies such as goal-directed fluid therapy (Rinehart et al., 2011), cardiopulmonary
79 management (Gholami et al., 2011), fluid resuscitation (Jin et al., 2019), and medically induced coma
80 (Yang and Shanechi, 2016; Liberman et al., 2013). In a similar way, and considering how irregular cortisol
81 secretion patterns affect energy state in patients with hypercortisolism, we leverage control theory in
82 regulating energy variations in these patients. While there exist medications effective in managing energy
83 levels, there is still a lack of closed-loop and automated architecture for making the decisions on the time
84 and dosage of the medications in real-time. Hence, we construct a virtual patient environment based on the
85 experimental cortisol data for further analysis. Then, we design the control algorithm that can determine
86 the time and dosage of hypothetical simulated medications in a real-time automated fashion.

87 As someone's energy variations are influenced by changes in their cortisol levels, the objective of
88 this research is to regulate the energy state by monitoring the cortisol secretion patterns. To model the
89 internal energy state and relate it to the cortisol variations, we utilize the state-space model presented in
90 (Wickramasuriya and Faghah, 2019b). To close the loop, we simulate hypothetical medication dynamics
91 and develop a control system. In the present simulation study, we apply hypothetical medication dynamics
92 as the actuation in a real-time closed-loop brain machine interface architecture (Azgomi and Faghah,
93 2019; Azgomi et al., 2019). As presented in Figure 1, a wearable device measures the cortisol data
94 in a non-invasive manner. We infer the CRH secretion times via a deconvolution algorithm (Pednekar
95 et al., 2020, 2019; Faghah, 2014; Faghah et al., 2014; Amin and Faghah, 2019b,a,c, 2018). We use the
96 state-space approach (Wickramasuriya and Faghah, 2019b; Brown et al., 2001) to link the CRH secretion
97 times, which cause the fluctuations in cortisol levels (Azgomi and Faghah, 2019; Wickramasuriya and
98 Faghah, 2019b; Faghah et al., 2015b; Wickramasuriya and Faghah, 2020a), to the internal energy state.
99 This state-space representation tracks the internal energy state continuously and provides the capability of
100 utilizing the control systems theory to close the loop. To estimate the hidden cognitive energy-related state
101 in real-time, we employ Bayesian filtering method (Wickramasuriya and Faghah, 2019b). By incorporating
102 hypothetical dynamical system model of medications effective in both decreasing and increasing energy
103 levels (Blockmans et al., 2006; James et al., 2007), and designing a fuzzy controller, we close the loop to
104 regulate the energy state in patients with hypercortisolism in a simulation environment.

105 In Section 2, we explain the steps required for creating the virtual patient environment. We also discuss
106 the state-space model along with the real-time estimation process. We then incorporate the hypothetical
107 medication dynamics and propose a knowledge-based control system to close the loop in real-time. In
108 Section 3, we present the outcome of implementing the proposed approach in regulating the energy state
109 in patients with hypercortisolism. More particularly, we present the results on two classes of patients: (1)
110 who do not have the circadian rhythm in their cortisol profiles, and (2) who have the circadian rhythm in
111 their cortisol profiles. The final results demonstrate that our proposed real-time architecture can not only
112 track one's energy state, but also regulate the energy variations in patients with hypercortisolism utilizing
113 the simulated medication dynamics. Section 4 points out the implications of our findings. This simulation
114 study based on the experimental data is the first step toward treating other hormone-related disorders.

2 METHODS

115 Figure 2 illustrates an overview of the proposed closed-loop architecture. The present study consists of two
 116 main parts: the offline process and the real-time closed-loop simulation environment. In the offline part,
 117 we first generate multi-day cortisol data for multiple subjects based on their experimental data collected
 118 over 24 hours. Although there are recent advances in monitoring cortisol levels using wearable devices
 119 (Parlak, 2021; Venugopal et al., 2011; Parlak et al., 2018), there is still a lack of technologies for real-time
 120 multi-day cortisol data collection. Hence, to design a virtual patient environment, we first follow the results
 121 from (Wickramasuriya and Faghah, 2019b; Brown et al., 2001; Lee et al., 2016) to simulate cortisol profiles
 122 in both healthy subjects and Cushing’s patients. To extend our preliminary results presented in (Azgomi
 123 and Faghah, 2019), we simulate data for ten subjects (Faghah, 2014). This offline process enables us to
 124 examine the performance of the proposed architecture in multiple cases. By performing deconvolution
 125 algorithm, we infer the cortisol secretion times and the circadian upper and lower envelopes. Utilizing
 126 Expectation Maximization (EM) approach, we estimate the circadian rhythm forcing function along with
 127 model parameters. In the offline stage, we also model dynamical systems for hypothetical medications with
 128 both inhibitory (i.e. medications to lower the cortisol levels) and excitatory (i.e. medications to elevate the
 129 cortisol levels) effects.

130 As depicted in the bottom section of Figure 2, we take the circadian rhythm forcing function in the
 131 real-time simulation system and relate the internal energy state to the cortisol secretion times and cortisol
 132 upper and lower bound envelopes using the state-space approach. Employing the Bayesian filtering,
 133 which uses the estimated model parameters calculated with the offline EM algorithm, we estimate the
 134 hidden energy-related state in real-time. Incorporating the dynamical system model of medications and the
 135 personalized desired levels of energy, we design a fuzzy controller to close the loop. The deigned control
 136 system will take the energy state estimate and determine the time and dosage of each medication as the
 137 actuation in the loop. Hence, it controls cortisol variations which will result in energy regulation.

138 2.1 Data Simulation

139 Due to the lack of multi-day experimental measurements of healthy subjects and the patients with
 140 Cushing’s disease, we first simulate multi-day cortisol data profiles (Wickramasuriya and Faghah, 2019b;
 141 Faghah, 2014; Brown et al., 2001; Lee et al., 2016). Following (Faghah et al., 2014; Brown et al., 2001),
 142 cortisol secretion process could be assumed to follow a second-order stochastic differential equation:

$$143 \frac{dCort_1(t)}{dt} = -\zeta_1 Cort_1(t) + n(t), \quad (1)$$

$$143 \frac{dCort_2(t)}{dt} = \zeta_1 Cort_1(t) - \zeta_2 Cort_2(t), \quad (2)$$

144 where $Cort_1(t)$ and $Cort_2(t)$ are cortisol concentration in adrenal glands and plasma space at time
 145 t , respectively (Faghah, 2014). Moreover, ζ_1 stands for cortisol infusion rate from adrenal gland to
 146 the blood, ζ_2 corresponds to the cortisol clearance rate by the liver (Faghah et al., 2014; Brown et al.,
 147 2001). In addition, $n(t)$ represents secretory events (pulses) underlying cortisol release. The output
 148 equation $y_k = Cort_2(k) + \psi_k$, where $Cort_2(k)$ is the discretized cortisol concentration in plasma with
 149 $\psi_k \sim \mathcal{N}(0, \sigma_\psi^2)$ as the measurement noise with variance σ_ψ^2 . We employ estimated model parameters ζ_1
 150 and ζ_2 derived in (Faghah et al., 2014). The details of this information are presented in supplementary
 151 information.

152 To model cortisol secretory events $n(t)$, we follow the approach presented in (Brown et al., 2001).

153 • Healthy Profiles: We use the gamma distribution for pulse inter-arrival times and Gaussian distribution
 154 for pulse amplitudes (Brown et al., 2001). The corresponding parameters for gamma distribution are
 155 $\alpha = 54$ and $\beta = 39$. The pulse amplitude follows a Gaussian distribution $H_k \sim \mathcal{N}(\mu_k, k_k^2)$, where
 156 $\mu_k = 6.1 + 3.93 \sin(\frac{2\pi k}{1440}) - 4.75 \cos(\frac{2\pi k}{1440}) - 2.53 \sin(\frac{4\pi k}{1440}) - 3.76 \cos(\frac{4\pi k}{1440})$ and $k_k = 0.1\sqrt{\mu_k}$
 157 (Azgomi and Faghah, 2019; Wickramasuriya and Faghah, 2019b).

158 To simulate the data for patients with Cushing's disease, we consider two cases: (1) Cushing's patients
 159 without circadian rhythms in their cortisol profiles, and (2) Cushing's patients with circadian rhythms in their
 160 cortisol profiles. While cortisol variations in patients with Cushing's disease do not follow normal circadian
 161 rhythms, at the very early stages of the disease, the circadian rhythms might be slightly dysregulated
 162 (Wickramasuriya and Faghah, 2019b; Van den Berg et al., 1995).

163 • Cushing's patients without circadian rhythm: We follow (Lee et al., 2016; Van den Berg et al., 1995)
 164 and consider the inter-arrival times following a gamma distribution that belong to the range of 59 ± 11
 165 min. Regarding the pulse amplitudes, we assume they are within the range of $38 \pm 2.5 \mu\text{gdL}^{-1} \text{min}^{-1}$,
 166 following a Gaussian distribution (Azgomi and Faghah, 2019; Wickramasuriya and Faghah, 2019b),
 167 • Cushing's patients with circadian rhythm: We employ $\mu_k = 38.5 + 1.93 \sin(\frac{2\pi k}{1440}) - 1.6 \cos(\frac{2\pi k}{1440}) -$
 168 $1.5 \sin(\frac{4\pi k}{1440}) - 3.5 \cos(\frac{4\pi k}{1440})$, $k_k = \frac{2.5}{\sqrt{38\mu_k}}$ as the Gaussian distribution parameters in the pulse
 169 amplitudes and the same gamma inter-arrival time distribution as described previously for the Cushing's
 170 patients with circadian rhythm.

171 Employing the model parameters ζ_1 and ζ_2 provided in supplementary information and a vector input of
 172 pulse timings and amplitudes $n(t)$ presented above, we simulate the cortisol profiles. We employ coupled
 173 differential equations (1) and (2), and add measurement noise to generate cortisol profile data for different
 174 subjects in three different situations. More particularly, we simulate the cortisol profiles associated with
 175 healthy subjects, Cushing's patients with circadian rhythm in their cortisol profiles and Cushing's patients
 176 without circadian rhythm in their cortisol profiles over five days for further analysis (Faghah, 2018, 2014;
 177 Brown et al., 2001). The resulting multi-day cortisol profiles are presented in supplementary information.
 178 As an example, the results associated with subject 1 are depicted in Figure 3.

179 2.2 State-space Modeling

180 Cortisol dynamical system explained above will generate the cortisol observations for our virtual patient
 181 environment. We employ the state-space approach presented in (Pednekar et al., 2019; Faghah, 2014) to
 182 relate the hidden cognitive energy-related state to cortisol variations. The state-space approach lets us
 183 systematically track internal energy state and control it in real-time (Smith et al., 2004). We model the
 184 cognitive energy-related state as the following first-order state-space representation:

$$x_k = \rho x_{k-1} + u_k + \epsilon_k + I_k, \quad (3)$$

185 where x_k is the hidden internal energy-related state, ρ is a person-specific parameter, u_k is the control
 186 input, $\epsilon_k \sim \mathcal{N}(0, \sigma_\epsilon^2)$ is the process noise, and I_k is being considered as the forcing function that keeps the
 187 energy variations during wakefulness and sleep in 24 hour periods. By analyzing the simulated cortisol
 188 profiles (Wickramasuriya and Faghah, 2019b), we design the following harmonic forcing function:

$$I_k = \sum_{i=1}^2 \alpha_i \sin\left(\frac{2\pi i k}{1440}\right) + \beta_i \cos\left(\frac{2\pi i k}{1440}\right), \quad (4)$$

189 where the coefficients α_i and β_i along with parameter ρ in (3) for each subject/case are derived using
 190 the EM algorithm explained in (Wickramasuriya and Faghah, 2019b). These parameters are presented in
 191 supplementary information.

192 Analyzing the discretized cortisol data at a one minute time resolution, we observe that the presence or
 193 absence of the cortisol pulses builds a binary point process (Wickramasuriya and Faghah, 2019b). Hence,
 194 we assume the probability of receiving pulses associated with CRH secretion times that results in cortisol
 195 secretion, c_k , follows a Bernoulli distribution:

$$P(c_k|p_k) = p_k^{c_k} (1 - p_k)^{1-c_k}, \quad (5)$$

196 where the probability p_k is connected to the energy state x_k by the following sigmoid function:

$$p_k = \frac{1}{1 + e^{-(\gamma_0 + \gamma_1 x_k)}}. \quad (6)$$

197 This model relates the probability p_k of observing a CRH pulse event c_k to the energy state x_k through
 198 person-specific baseline parameters γ_0 and γ_1 calculated by the offline EM.

In addition to the cortisol secretion times as binary observations, we use the upper and the lower bound envelopes of the blood cortisol measurements as continuous observations to estimate the energy state x_k (Wickramasuriya and Faghah, 2019b). We label these two upper and lower envelopes as R_k and S_k , respectively. Assuming there exists a linear relationship between these envelopes and the corresponding state x_k :

$$R_k = r_0 + r_1 x_k + v_k, \quad (7)$$

$$S_k = s_0 + s_1 x_k + w_k, \quad (8)$$

199 where $v_k \sim \mathcal{N}(0, \sigma_v^2)$, $w_k \sim \mathcal{N}(0, \sigma_w^2)$, and r_0, r_1, s_0, s_1 are regression coefficients obtained by offline
 200 EM algorithm (Wickramasuriya and Faghah, 2019b, 2020b,a).

201 It is worth mentioning that while there exist recent advances in performing deconvolution methods, there
 202 is still lack of real-time deconvolution algorithm. With real-time deconvolution tool, we directly infer the
 203 cortisol impulses $n(t)$ in (1) and employ it in further analysis.

204 2.3 Energy State Estimation

205 We employ two continuous and one binary observations in the estimation process (Coleman et al., 2011;
 206 Prerau et al., 2009; Wickramasuriya and Faghah, 2019a). Taking the CRH pulse events c_k and the upper
 207 and lower envelopes R_k and S_k as observations, we perform Bayesian filtering (Coleman et al., 2011;
 208 Wickramasuriya and Faghah, 2020b) to estimate the hidden cognitive energy-related state mean x_k and its
 209 variance σ_k in two prediction and update steps:

- Prediction step:

$$x_{k|k-1} = \rho x_{k-1|k-1} + I_k + u_k, \quad (9)$$

$$\sigma_{k|k-1}^2 = \rho^2 \sigma_{k-1|k-1}^2 + \sigma_\epsilon^2. \quad (10)$$

- Update step:

$$A_k = \frac{\sigma_{k|k-1}^2}{\sigma_v^2 \sigma_w^2 + \sigma_{k|k-1}^2 (r_1^2 \sigma_w^2 + s_1^2 \sigma_v^2)}, \quad (11)$$

$$\begin{aligned} \hat{x}_k = x_{k|k} = x_{k|k-1} + A_k & \left(\gamma_1 \sigma_v^2 (c_k - p_k) \right. \\ & + r_1^2 \sigma_w^2 (R_k - r_0 - r_1 x_{k|k-1}) \\ & \left. + s_1^2 \sigma_v^2 (S_k - s_0 - s_1 x_{k|k-1}) \right), \end{aligned} \quad (12)$$

$$\hat{\sigma}_k^2 = \sigma_{k|k}^2 = \left(\frac{1}{\sigma_{k|k-1}^2} + \gamma_1^2 p_k (1 - p_k) + \frac{r_1^2}{\sigma_v^2} + \frac{s_1^2}{\sigma_w^2} \right)^{-1}. \quad (13)$$

210 The p_k presented in (12) is related to the \hat{x}_k by (6). Consequently, the \hat{x}_k is present on both sides of (12)
211 and we employ Newton's method to solve the update equations.

212 2.4 Dynamic System Model of Medications

The next step in closing the loop and regulating energy-related state is to model the dynamical system of hypothetical medications and include them in control design process. In this research, we focus on the medications that can lead the subjects to reach their desired energy levels (Blockmans et al., 2006; James et al., 2007). In this regard, we consider two classes of medications: (1) for elevating the energy levels required for daily activity (i.e. excitation effect), and (2) for helping the subjects to lower their energy levels in the evening which may help them experience well-ordered sleep cycles at nights (i.e. inhibition effect). To analyze how a specific medication affects one's energy levels and incorporate them in the control design process, we model their dynamics by a second-order state-space representation:

$$\begin{bmatrix} \dot{z}_1(t) \\ \dot{z}_2(t) \end{bmatrix} = \begin{bmatrix} -\theta_{i1} & 0 \\ \theta_{i1} & -\theta_{i2} \end{bmatrix} \begin{bmatrix} z_1(t) \\ z_2(t) \end{bmatrix} + \begin{bmatrix} \eta \\ 0 \end{bmatrix} q(t), \quad (14)$$

where $i = 1, 2$ denotes the type of medications. $y(t) = z_2(t)$ is the estimated energy level and θ_{i1}, θ_{i2} correspond the infusion rate and the clearance rate of each corresponding medication i , respectively. We assume $\theta_i = [\theta_{i1} \ \theta_{i2}]$. In the state-space representation (14), $q(t) = q_i^* \delta(t - \tau_i^*)$ is the actuation input impulses where parameters τ_i^* and q_i^* stand for time and dosage of the corresponding medication i (Faghih, 2014; Faghih et al., 2015a). The η term also determines if the actuation should be excitation (i.e. $\eta = +1$ for elevating the energy level) or inhibition (i.e. $\eta = -1$ for lowering the energy level). With this representation, we analyze how using a specific dosage q_i^* of medication i at time τ_i^* will affect the internal energy levels $z_2(t)$ dynamically. Solving the state-space equation (14) and considering the output equation $y(t) = z_2(t)$, we compute the output at each time step j as:

$$y_j = a_j y_0 + \mathbf{b}_j \mathbf{q} + e_j. \quad (15)$$

213 where $a_j = e^{-\theta_{i2} j}$ and $\mathbf{b}_j = \frac{\theta_{i1}}{\theta_{i1} - \theta_{i2}} [(e^{-\theta_{i2} j} - e^{-\theta_{i1} j}) \quad (e^{-\theta_{i2}(j-1)} - e^{-\theta_{i1}(j-1)}) \quad \dots \quad (e^{-\theta_{i2}} - 214 e^{-\theta_{i1}}) \quad \underbrace{0 \quad \dots \quad 0}_{N-j}]'$. The vector input \mathbf{q} consists of one non-zero element (i.e. $\mathbf{q} = [q_1 \dots q_N]$, where

215 $q_j = 0, \forall j$ except the one element q_i^* at time τ_i^*) and error term $e_j \sim \mathcal{N}(0, \sigma_e^2)$. Forming the output for
 216 the whole time horizon N , we generate the vector representation \mathbf{y} as the observation:

$$\mathbf{y} = \mathbf{A}_\theta y_0 + \mathbf{B}_\theta \mathbf{q} + \mathbf{e}, \quad (16)$$

217 where $\mathbf{y} = [y_1 \ y_2 \ \dots \ y_N]'$, $\mathbf{A}_\theta = [a_1 \ a_2 \ \dots \ a_N]'$, $\mathbf{B}_\theta = [b_1 \ b_2 \ \dots \ b_N]'$, and
 218 $\mathbf{e} = [e_1 \ e_2 \ \dots \ e_N]'$. To complete the system identification task, we impose the constraint $\|\mathbf{q}\|_0 = 1$
 219 in the corresponding parameter estimation problem (Dahleh et al., 2004). To find the optimum parameters,
 220 we solve the following optimization problem to optimize the error term $J = \mathbf{e}'\mathbf{e}$:

$$\min_{\theta_i, \mathbf{q}} J = \frac{1}{2} \|\mathbf{y} - \mathbf{A}_\theta y_0 - \mathbf{B}_\theta \mathbf{q}\|_2^2, \quad (17)$$

$$\|\mathbf{q}\|_0 = 1$$

221 Given \mathbf{y} , we can estimate \mathbf{A}_θ , \mathbf{B}_θ (i.e. include θ_i), and \mathbf{q} to obtain the actuation dynamics (Faghah et al.,
 222 2015b). As a result of this process, we simulate the way that a specific medication affects the energy levels.
 223 In the following part, we explain the control approach and close the loop.

224 In this *in silico* study, incorporating the hypothetical medication dynamics (14), we design the control
 225 strategy to determine the time and the dosage of each medication to regulate the estimated energy state. In
 226 the practical case, this system identification step is recommended to be performed in parallel to update the
 227 dynamical model parameters in real-time.

228 2.5 Fuzzy Control System

229 Fuzzy control, which is known as a knowledge-based control approach, employs the insights about the
 230 system, performs the corresponding inference, and makes the control decisions (Garibaldi and Ozen, 2007;
 231 Mendes et al., 2019; Yu et al., 2020). As an intelligent approach, it is a powerful bridge from the expertise
 232 inference to the real world (Azgomi et al., 2019; Lin et al., 2018). Any fuzzy controller includes four main
 233 parts: rule base, fuzzifier, inference engine, and defuzzifier. In the rule base, we define the rules to achieve
 234 our control objective (Zoukit et al., 2019). These IF-THEN rules are derived employing expert knowledge
 235 of the system and the corresponding constraints.

236 In the present study, the estimated cognitive energy-related state and the time of the day are the inputs of
 237 the fuzzy controller, and the control output is the time and dosage of the required simulated medications
 238 (Azgomi and Faghah, 2019). To design the fuzzy system, we employ information about the personalized
 239 levels of energy state and the dictionary of medication dosages and actuation responses (Figure 2). We
 240 also use two classes of actuation: exciting medications which increase the energy levels, and inhibiting
 241 medications which lower the estimated energy levels. The purpose of applying medications with exciting
 242 and inhibiting effects is to provide the required energy for daily activity (Pednekar et al., 2020) and lowering
 243 the energy-related state to result in a better sleep cycle at nights (Feeiders et al., 2019), respectively. Based
 244 on the literature and nature of the medications (Blockmans et al., 2006; James et al., 2007), we consider the
 245 constraint of applying maximum two medications (i.e. control inputs) per day: one in the morning which
 246 increases energy levels, and one in the evening to lower the energy levels. The rule base of the proposed
 247 fuzzy controller is presented in Table 1.

248 As an example, to clarify the structure of rules presented in Table 1, rule number 1 denotes:

249 • If the estimated energy state is *High*, and the time is *early in the morning* then the actuation is *positive*
 250 *small*.

251 To quantify the linguistic variables presented in the rule base, we employ membership functions as the
 252 fuzzifiers (Azgomi et al., 2013). Investigating the simulated environment including estimated energy state,
 253 hypothetical medication dynamics, personalized levels of energy state, and the rule base, we utilize the
 254 appropriate number of relevant membership functions presented in Figure 4. As observed in Figure 4, we
 255 employ six membership functions for time of the day (input 1), three membership functions for estimated
 256 energy values (input 2), and seven membership functions for the control output to cover all cases in the
 257 rule base (Table 1).

258 We use *Mamdani* inference engine to execute the inference and produce fuzzy outputs (Zulfikar et al.,
 259 2018). We employ *minimum* method for both *AND* operation in the fuzzy inputs and implication process
 260 for fuzzy output generation. We also use *Maximum* method for rule output aggregation. Consequently, the
 261 final fuzzy output will be resulted as:

$$\mu_{mamdani}(q) = \mu_m(q) = \max_j [\mu_j(q)] = \max_j [\min(\min(\mu_{time}(t), \mu_{state}(x)), \mu_{actuation}(c))] = \\ \max_j [\min(\mu_{time}(t), \mu_{state}(x), \mu_{actuation}(c))]. \quad (18)$$

262 where j denotes the effective rules at each time step and $\mu_j(q)$ is the resulted fuzzy set. $\mu_{time}(t)$, $\mu_{state}(x)$,
 263 and $\mu_{actuation}(c)$ also stand for the membership functions presented in Figure 4. To demonstrate the way
 264 that this inference engine works, we explain the proposed fuzzy system (18). At each time step, the fuzzy
 265 system monitors all the rules presented in Table 1 and finds the effective rules according to the input
 266 membership functions (Figure 4). By extracting the corresponding membership degree and executing *AND*
 267 operation in each applied rule, it then performs implication between the resulted input fuzzy sets (time
 268 and the estimated energy state) and the corresponding output fuzzy membership function (medication
 269 actuation). By aggregating results from all applied rules, it generates the final fuzzy output. To produce
 270 crisp output out of the generated fuzzy outputs and applying it into the system in real-time, we employ
 271 *centroid* defuzzification method:

$$q^* = \frac{\int \mu_m(q) \cdot q \, dq}{\int \mu_m(q) \, dq}. \quad (19)$$

272 At any time step where either the rules with *Zero* actuation output (Table 1) are effective, or the output q^*
 273 in (19) equals zero, the fuzzy system would determine no need for applied control. At the time t that the
 274 fuzzy system results a nonzero output ($q^* \neq 0$), time of actuation would be derived ($\tau^* = t$). Considering
 275 the resulted crisp output and constraint to apply maximum two medications per day, the designed control
 276 will determine the time and the amplitudes of each medication. Hence, by taking the decisions about the
 277 dosage and the desired time of the hypothetical medications (i.e., q^* and τ^* in (14)), the resulted control
 278 signal (i.e., u_k in (3)) will be applied to regulate the internal energy state.

3 RESULTS

279 In this section, first we present the open-loop results. Then, we present our real-time closed-loop results for
 280 two categories of Cushing's diseases: one without circadian rhythm in their cortisol profiles, and another
 281 with circadian rhythm in their cortisol profiles. The results associated with ten simulated subjects are
 282 presented in Figures 5-7.

283 3.1 Open-loop (Healthy subject)

284 In the first part, we use data associated with healthy subjects to show the tracking performance. As
 285 depicted in the left panels of Figures 5-7, the system tracks the energy state in an open-loop manner. In the

286 middle sub-panel, it is observed that there is not any control in this stage ($u_k = 0$). Top sub-panels show
 287 that the estimated energy state has its peak during the daytime (06:00 - 16:00) and it drops in the evening.
 288 It verifies that we successfully track the energy state in the simulated healthy profiles.

289 **3.2 Closed-loop (Cushing's patients without circadian rhythm)**

290 In this part, we employ the simulated cortisol data associated with Cushing's patients without circadian
 291 rhythm in their cortisol profiles. The results are observed in the middle panels of Figures 5-7. The white
 292 and grey backgrounds correspond to the open-loop and the closed-loop periods, respectively. After day
 293 two, the control is activated and the closed-loop system detects an imbalanced energy state (top sub-panel
 294 in the middle panels of Figures 5-7). Then, the time and dosage of the required simulated medications are
 295 produced by the control system (bottom sub-panel in the middle panels of Figures 5-7). The red pulses
 296 stand for the simulated medications with excitation effects, while the blue pulses are associated with the
 297 simulated medications with inhibitory effects. Employing the suggested hypothetical medications will
 298 lead the generated control input to follow the curves presented in the middle sub-panel of Figures 5-7.
 299 Thereafter, starting day three of simulation (once the loop gets closed), the energy state is being regulated.

300 **3.3 Closed-loop (Cushing's patients with circadian rhythm)**

301 Similar to the previous case, here we investigate the performance of the proposed closed-loop architecture
 302 by making use of simulated Cushing's patients' data together with existing circadian rhythm in their cortisol
 303 profiles. The results are presented in the right panels of Figures 5-7. Similarly, the system detects the
 304 irregular energy patterns and regulates the energy state variations by designing the corresponding control
 305 signals in a closed-loop manner.

4 DISCUSSION AND CONCLUSIONS

306 Inspired by the fact that CRH plays an undeniable role in internal energy regulation, we proposed our novel
 307 approach for regulating the energy-related state using a wearable brain machine interface architecture.
 308 In the proposed architecture, we infer one's energy variations by monitoring cortisol data which can be
 309 collected using wearable devices in real time (Parlak et al., 2018). We implemented the control algorithm
 310 on ten simulated data profiles in healthy subjects and Cushing's patients.

311 In the offline stage of this research, we simulated the cortisol data for multiple subjects. As it is validated
 312 in the literature, we employ stochastic models to simulate multi-day cortisol secretion patterns. Following
 313 (Brown et al., 2001; Faghah, 2014; Lee et al., 2016; Wickramasuriya and Faghah, 2019b), we consider
 314 different gamma distributions for inter-arrival times associated with cortisol secretion impulses. We also
 315 assume the pulse amplitudes follow Gaussian distributions. Employing the model parameters that are
 316 presented in the manuscript, we simulate cortisol profiles which have day-by-day variability. The stochastic
 317 variability existing in model parameters would be viewed as a realistic multi-day case in this *in silico* study.
 318 Employing the state-space approach along with EM algorithm, we estimated the model parameters and the
 319 forcing circadian function. Using the virtual patient environment, we aimed to track the energy state based
 320 on the changes in cortisol secretion times and cortisol upper and lower envelopes (See Figure 2).

321 With the goal of tracking the energy state in the proposed architecture, we first simulated a real-time
 322 open-loop case. In this part, we used the data associated with healthy subjects. In the present study, due to
 323 the lack of real-time deconvolution algorithm, we assume the presence or absence of cortisol secretion
 324 forms a binary point process and follows a Bernoulli distribution. Besides, we take the cortisol upper
 325 and lower bound envelopes as the continuous observations. Utilizing the EM algorithm, we estimated the
 326 hidden energy state. As it can be seen in the left panels, with no control implemented (i.e. $u_k = 0$), the
 327 energy state variations in simulated healthy profiles are as desired. It is observed that the energy state is

328 at its peak during the daytime and it drops in the evening. It leads to providing enough energy for daily
329 activity and having well-ordered sleep cycles at evening. In fact, this normal condition is because of the
330 well-balanced cortisol secretion patterns in healthy subjects.

331 In this research, we assumed that including the hypothetical medications would impact the energy state.
332 Hence, we incorporated the simulated medication dynamics as the actuation while closing the loop. In this
333 regard, we first presented the system identification required to design the control system. To incorporate
334 the corresponding medications in real-world implementation of the proposed closed-loop architectures, it
335 is important to pay appropriate attention to medications' half-lives. In the present design, we assumed that
336 the hypothetical medications have prompt effects on one's energy levels. In the case of utilizing long-acting
337 agents, the rules and membership functions should be revised accordingly. While this step is performed
338 in the offline stage of this research, in the practical case, it is recommended to execute it in real-time to
339 update the medication dynamics according to the subject's response. To design the control, we proposed
340 a knowledge-based fuzzy controller. Employing the estimated energy state, personalized desired levels
341 of energy state, and hypothetical medication dynamics we built the rule base, membership functions, and
342 inference engine (See Figure 2).

343 Next, we presented the results of the closed-loop system. In this regard, we employed the cortisol data
344 profiles associated with the Cushing's patients. To depict the performance of the closed-loop system, we
345 assumed the control system gets activated starting day three, which means the system is open-loop (i.e.
346 $u_k = 0$) in the first two days of the simulation. During the open-loop period, we observe that the energy
347 variations do not follow the ideal circadian rhythm. In other words, the patients with hypercortisolism do
348 not have normal cortisol secretion patterns which will cause them to have insufficient energy levels in the
349 day time and experience disturbed sleep cycles at night (Pednekar et al., 2020). Starting day three, the
350 feedback control system (i.e. $u_k \neq 0$) closes the loop (grey background in Figures 5-7). In the closed-loop
351 period, the implemented control system detects undesired energy variations and tries to infer the right
352 time and dosage of the simulated medications in real-time. That is to say, the fuzzy structure receives the
353 estimated energy state, employs the rule base (Table 1) and membership functions (Figure 4), and generates
354 the appropriate control signal. This intermittent control signal is depicted in the bottom sub-panels of
355 Figures 5-7. When low levels of energy are detected, the red pulses would be generated to adjust the dosage
356 of the required medications with excitation effect to provide required energy levels. On the other hand,
357 once undesired high levels of energy are detected in the evening, the medications with the energy lowering
358 effect, i.e. blue pulses, would be suggested to provide the inhibition effect. The required time and dosage
359 of these hypothetical medications are produced by the fuzzy structure. The control actuation signal, which
360 is result of applying these simulated medications, is presented in the middle sub-panels of Figures 5-7.
361 Considering the constraint of using maximum two medications per day (Bouwer et al., 2000), the energy
362 state is regulated in real-time. It is worth mentioning that in the real-world case, the only needed signal
363 for closing the loop is the time and dosage of required medications. Since this simulation study is the first
364 step to show the feasibility of our proposed approach, we simulated hypothetical medication dynamics to
365 include actuation in the virtual patient environment.

366 In the final part of our results, we presented the outcomes of our proposed structure on simulated cortisol
367 data profiles associated with the Cushing's patients with circadian rhythm in their profiles. While Cushing's
368 patients do not generally have the required circadian rhythm in their cortisol profiles, there exist some
369 patients with some circadian rhythm in their blood cortisol profiles (Lee et al., 2016). This slight circadian
370 rhythm could be assumed to be available in the patients in their early stages of Cushing's disease. Similar

371 to the results of the Cushing's patients without circadian rhythm, our proposed closed-loop architecture
372 successfully detects the energy irregularities and makes the control decisions in real time.

373 Analyzing the results of multiple subjects, we observe some interesting outcomes. In the results associated
374 with subjects 1, 5, 6, 7 and 10, we see that for some days no blue pulses (i.e. simulated medications with
375 the inhibition effects) are necessary. It might be because energy levels are already low and would not
376 affect their sleep cycles. In these cases, employing only the medications with excitation effects in the
377 morning may lead to energy regulation in the evening too. These results are shreds of evidence of an
378 intrinsic advantage of our proposed closed-loop architectures which is handling the energy regulation in an
379 automated way and suggesting the medications as needed.

380 To further depict the efficiency of the proposed closed-loop architecture, we define corresponding metrics
381 (Figures 8-9). As the first criteria, we analyze the effect of closed-loop system in increasing the difference
382 between average levels of energy in the day and night (top panel of Figure 8). As presented, the difference
383 between the average levels of energy in day and night has been increased for all ten simulated subjects
384 in both Cushing's classes (filled green circles compared to the empty circles). As the second criteria, we
385 analyzed the growth of internal energy state in the morning, which will ultimately lead the subjects to wake
386 up with higher levels of energy. To do this task, we compared the growth of energy before the start of the
387 day in both open-loop and closed-loop cases (middle panel of Figure 8). The observed growth of energy in
388 all simulated subjects will help them to wake up with having more energy required for their daily activities.
389 As the final criteria, we compared the drop of energy levels late at evening (bottom panel of Figure 8). It
390 demonstrates how the proposed closed-loop architecture resulted in decreasing the energy levels required
391 for a better sleep cycle. As presented in the bottom panel of Figure 8, the internal energy state in patients
392 with Cushing's disease are not decreased sufficiently in the evenings (empty circles). However, in the
393 closed-loop case, by applying the required medications, the simulated energy state has been dropped more
394 efficiently which will further help the subjects to experience more balanced sleep cycle at night.

395 Analyzing the results on all the simulated subjects, the difference between the average energy levels in
396 day and night in Cushing's patients without and with circadian rhythm in their cortisol profiles is improved
397 by 140% and 97%, respectively (left sub-panels in Figure 9). The growth in the energy levels before
398 the wake time in both classes of Cushing's patients is improved by 245% and 75%, respectively (middle
399 sub-panels in Figure 9). Similarly, the average drop in the energy levels required for sleep time regulation
400 is improved by 473% and 208% in simulated Cushing's patients without and with circadian rhythm in
401 their profiles has been, respectively (right sub-panels in Figure 9). This analysis verify how our proposed
402 architecture is effective in regulating energy levels in a virtual patient environment.

403 In the offline stage of this research, we simulated multi-day data profiles for healthy subjects and subjects
404 with Cushing's disease. It is worth mentioning that this stage of simulating multi-day data profiles is because
405 of the lack of technology for real-time cortisol measurements. Future advances in wearable technologies
406 would provide the opportunity to continuously monitor the cortisol data and design a system that could
407 take care of inter- and intra-subjects fluctuations. In the present study, we assumed that the suggested
408 medications could be successful in lowering or increasing energy levels. In practical implementation, there
409 exist multiple factors that might cause the proposed architectures (i.e., using suggested medications to
410 regulate internal energy state) to fail and result in less efficiency.

411 • Diverse sensitivity to glucocorticoid hormones among individuals might prevent to observe similar
412 energy adjustments in response to the medications (Inda et al., 2017).

413 • Sever dysregulation of the HPA axis, which happens in some endogenous Cushing's syndrome cases,
414 could only be treated by removing the pituitary or adrenal tumor(s) (Nieman et al., 2015).

415 Implementing the proposed wearable brain machine interface architecture on multiple simulated cortisol
416 profiles, we demonstrated that we can reach energy regulation in hypercortisolism. Simulated results verify
417 that the proposed closed-loop approach has great potential to be utilized in real life. In the prospective
418 practical system, a real-time deconvolution algorithm should be utilized to derive the CRH secretion times.
419 Employing the proposed approach, in addition to taking advantage of wearable devices, which may monitor
420 blood cortisol levels in real-time, the time and dosage of the required medications would be regulated in a
421 closed-loop automated manner. Since the cortisol variations are influenced by a variety of physiological
422 and psychological factors, a future direction of this research could be including additional information from
423 multiple sources while designing the closed-loop system. In the prospective architectures, a multi-input
424 multi-output system will take the information from multiple sources and make the required decisions about
425 taking the medications (i.e., dosage and time). It results in an increase in medications' efficiency and
426 minimize their possible side effects. Future directions of this research could be incorporating all possible
427 medications and designing the control algorithms with the capability to choose among them. Another
428 possible future direction could be including the system identification process for each medication inside
429 the real-time system. As a result, the way that each specific person responds to a particular medication
430 will be monitored to update the medication dynamics in real-time. Consequently, the personalized control
431 design would be more efficient.

ACKNOWLEDGMENTS

432 This paper was presented in part at the proceedings of the Asilomar Conference on Signals, Systems, and
433 Computers (Azgomi and Faghah, 2019).

AUTHOR CONTRIBUTIONS

434 RF conceived and designed the study. RF and HF developed the algorithms and analysis tools. HF
435 performed research, analyzed data, and wrote the manuscript. HF, JH, and RF revised the manuscript.

DATA AVAILABILITY STATEMENT

436 The original contributions presented in the study are included in the article/supplementary material, further
437 inquiries can be directed to the corresponding author.

FUNDING

438 This work was supported in part by NSF CAREER Award4441942585 – MINDWATCH: Multimodal
439 Intelligent Noninvasive brain state Decoder for Wearable AdapTive445Closed-loop arcHitectures and NSF
440 grant 1755780 – CRII: CPS: Wearable-Machine Interface Architectures.

CONFLICT OF INTEREST STATEMENT

441 HF and JH declare that the research was conducted in the absence of any commercial or financial
442 relationships that could be construed as a potential conflict of interest. RF is a co-inventor on a provisional
443 patent that designs decoders for estimating energy based on cortisol observations.

REFERENCES

444 Amin, M. R. and Faghah, R. T. (2018). Inferring autonomic nervous system stimulation from hand and
445 foot skin conductance measurements. In *2018 52nd Asilomar Conference on Signals, Systems, and*
446 *Computers* (IEEE), 655–660, (Pacific Grove, CA).

447 Amin, M. R. and Faghah, R. T. (2019a). Robust inference of autonomic nervous system activation using
448 skin conductance measurements: A multi-channel sparse system identification approach. *IEEE Access* 7,
449 173419–173437

450 Amin, M. R. and Faghah, R. T. (2019b). Sparse deconvolution of electrodermal activity via continuous-time
451 system identification. *IEEE Transactions on Biomedical Engineering* 66, 2585–2595

452 Amin, M. R. and Faghah, R. T. (2019c). Tonic and phasic decomposition of skin conductance data: A
453 generalized-cross-validation-based block coordinate descent approach. In *2019 41st Annual International*
454 *Conference of the IEEE Engineering in Medicine and Biology Society (EMBC)* (IEEE), 745–749,
455 (Berlin).

456 Arnold, L. M. (2008). Understanding fatigue in major depressive disorder and other medical disorders.
457 *Psychosomatics* 49, 185–190

458 Azgomi, H. F. and Faghah, R. T. (2019). A wearable brain machine interface architecture for regulation of
459 energy in hypercortisolism. In *2019 53rd Asilomar Conference on Signals, Systems, and Computers*
460 (IEEE), 254–258, (Pacific Grove, CA).

461 Azgomi, H. F., Poshtan, J., and Poshtan, M. (2013). Experimental validation on stator fault detection
462 via fuzzy logic. In *Electric Power and Energy Conversion Systems (EPECS), 2013 3rd International*
463 *Conference on* (IEEE), 1–6, (Istanbul).

464 Azgomi, H. F., Wickramasuriya, D. S., and Faghah, R. T. (2019). State-space modeling and fuzzy feedback
465 control of cognitive stress. In *2019 41st Annual International Conference of the IEEE Engineering in*
466 *Medicine and Biology Society (EMBC)* (IEEE), 6327–6330, (Berlin).

467 Björntorp, P. and Rosmond, R. (2000). Obesity and cortisol. *Nutrition* 16, 924–936

468 Blockmans, D., Persoons, P., Van Houdenhove, B., and Bobbaers, H. (2006). Does methylphenidate reduce
469 the symptoms of chronic fatigue syndrome? *The American journal of medicine* 119, 167–e23

470 Bouwer, C., Claassen, J., Dinan, T. G., and Nemeroff, C. B. (2000). Prednisone augmentation in treatment-
471 resistant depression with fatigue and hypocortisolism: A case series. *Depression and anxiety* 12,
472 44–50

473 Brown, E. N., Meehan, P. M., and Dempster, A. P. (2001). A stochastic differential equation model
474 of diurnal cortisol patterns. *American Journal of Physiology-Endocrinology And Metabolism* 280,
475 E450–E461

476 Chaudhuri, A. and Behan, P. O. (2004). Fatigue in neurological disorders. *The lancet* 363, 978–988

477 Coleman, T. P., Yanike, M., Suzuki, W. A., and Brown, E. N. (2011). A mixed-filter algorithm for
478 dynamically tracking learning from multiple behavioral and neurophysiological measures. *The dynamic*
479 *brain: An exploration of neuronal variability and its functional significance* , 1–16

480 Crofford, L. J., Young, E. A., Engleberg, N. C., Korszun, A., Brucksch, C. B., McClure, L. A., et al. (2004).
481 Basal circadian and pulsatile acth and cortisol secretion in patients with fibromyalgia and/or chronic
482 fatigue syndrome. *Brain, behavior, and immunity* 18, 314–325

483 Dahleh, M., Dahleh, M. A., and Verghese, G. (2004). Lectures on dynamic systems and control. *A+ A* 4,
484 1–100

485 Driessens, N., Maiter, D., Borensztein, P., Jaspart, A., Bostnavaron, M., and Beckers, A. (2018). Long-term
486 treatment with metyrapone in four patients with cushing's disease

487 Dwyer, R. T., Gifford, R. H., Bess, F. H., Dorman, M., Spahr, A., and Hornsby, B. W. (2019). Diurnal
488 cortisol levels and subjective ratings of effort and fatigue in adult cochlear implant users: A pilot study.
489 *American journal of audiology* 28, 686–696

490 D'Angelo, V., Beccuti, G., Berardelli, R., Karamouzis, I., Zichi, C., Giordano, R., et al. (2015). Cushing's
491 syndrome is associated with sleep alterations detected by wrist actigraphy. *Pituitary* 18, 893–897

492 Faghih, R. T. (2014). *System identification of cortisol secretion: Characterizing pulsatile dynamics*. Ph.D.
493 thesis, Massachusetts Institute of Technology

494 Faghih, R. T. (2018). From physiological signals to pulsatile dynamics: a sparse system identification
495 approach. In *Dynamic Neuroscience* (Springer). 239–265. doi:10.1007/978-3-319-71976-4_10

496 Faghih, R. T., Dahleh, M. A., Adler, G. K., Klerman, E. B., and Brown, E. N. (2014). Deconvolution of
497 serum cortisol levels by using compressed sensing. *PloS one* 9

498 Faghih, R. T., Dahleh, M. A., Adler, G. K., Klerman, E. B., and Brown, E. N. (2015a). Quantifying
499 pituitary-adrenal dynamics and deconvolution of concurrent cortisol and adrenocorticotropic hormone
500 data by compressed sensing. *IEEE Transactions on Biomedical Engineering* 62, 2379–2388

501 Faghih, R. T., Dahleh, M. A., and Brown, E. N. (2015b). An optimization formulation for characterization
502 of pulsatile cortisol secretion. *Frontiers in neuroscience* 9, 228

503 Feelders, R. A., Newell-Price, J., Pivonello, R., Nieman, L. K., Hofland, L. J., and Lacroix, A. (2019).
504 Advances in the medical treatment of cushing's syndrome. *The Lancet Diabetes & Endocrinology* 7,
505 300–312

506 Fleseriu, M., Petersenn, S., Biller, B. M., Kadioglu, P., De Block, C., T'Sjoen, G., et al. (2019). Long-term
507 efficacy and safety of once-monthly pasireotide in cushing's disease: A phase iii extension study. *Clinical
508 endocrinology* 91, 776–785

509 Garibaldi, J. M. and Ozen, T. (2007). Uncertain fuzzy reasoning: a case study in modelling expert decision
510 making. *IEEE Transactions on Fuzzy Systems* 15, 16–30

511 Gholami, B., Bailey, J. M., Haddad, W. M., and Tannenbaum, A. R. (2011). Clinical decision support
512 and closed-loop control for cardiopulmonary management and intensive care unit sedation using expert
513 systems. *IEEE transactions on control systems technology* 20, 1343–1350

514 Hakamata, Y., Komi, S., Moriguchi, Y., Izawa, S., Motomura, Y., Sato, E., et al. (2017). Amygdala-centred
515 functional connectivity affects daily cortisol concentrations: a putative link with anxiety. *Scientific
516 reports* 7, 1–11

517 Harris, A., Reme, S. E., Tangen, T., Hansen, Å. M., Garde, A. H., and Eriksen, H. R. (2015). Diurnal
518 cortisol rhythm: Associated with anxiety and depression, or just an indication of lack of energy?
519 *Psychiatry research* 228, 209–215

520 Inda, C., Armando, N. G., dos Santos Claro, P. A., and Silberstein, S. (2017). Endocrinology and the brain:
521 corticotropin-releasing hormone signaling. *Endocrine connections* 6, R99–R120

522 James, F. O., Cermakian, N., and Boivin, D. B. (2007). Circadian rhythms of melatonin, cortisol, and clock
523 gene expression during simulated night shift work. *Sleep* 30, 1427–1436

524 Jin, X., Bighamian, R., and Hahn, J.-O. (2019). Development and in silico evaluation of a model-based
525 closed-loop fluid resuscitation control algorithm. *IEEE Transactions on Biomedical Engineering* 66,
526 1905–1914

527 Lee, M. A., Bakh, N., Bisker, G., Brown, E. N., and Strano, M. S. (2016). A pharmacokinetic model of a
528 tissue implantable cortisol sensor. *Advanced healthcare materials* 5, 3004–3015

529 Liberman, M. Y., Ching, S., Chemali, J., and Brown, E. N. (2013). A closed-loop anesthetic delivery
530 system for real-time control of burst suppression. *Journal of neural engineering* 10, 046004

531 Lin, H.-R., Cao, B.-Y., and Liao, Y.-z. (2018). Fuzzy control. In *Fuzzy Sets Theory Preliminary* (Springer).
532 73–108. doi:10.1007/978-3-319-70749-5_3

533 Mendes, W. R., Araújo, F. M. U., Dutta, R., and Heeren, D. M. (2019). Fuzzy control system for variable
534 rate irrigation using remote sensing. *Expert systems with applications* 124, 13–24

535 Nieman, L. K., Biller, B. M., Findling, J. W., Murad, M. H., Newell-Price, J., Savage, M. O., et al. (2015).
536 Treatment of cushing's syndrome: an endocrine society clinical practice guideline. *The Journal of
537 Clinical Endocrinology & Metabolism* 100, 2807–2831

538 Nieuwenhuizen, A. G. and Rutters, F. (2008). The hypothalamic-pituitary-adrenal-axis in the regulation of
539 energy balance. *Physiology & behavior* 94, 169–177

540 Parlak, O. (2021). Portable and wearable real-time stress monitoring: A critical review. *Sensors and
541 Actuators Reports* 3, 100036

542 Parlak, O., Keene, S. T., Marais, A., Curto, V. F., and Salleo, A. (2018). Molecularly selective nanoporous
543 membrane-based wearable organic electrochemical device for noninvasive cortisol sensing. *Science
544 advances* 4, eaar2904

545 Pednekar, D. D., Amin, M. R., Azgomi, H. F., Aschbacher, K., Crofford, L. J., and Faghah, R. T. (2019). A
546 system theoretic investigation of cortisol dysregulation in fibromyalgia patients with chronic fatigue. In
547 *2019 41st Annual International Conference of the IEEE Engineering in Medicine and Biology Society
548 (EMBC)* (IEEE), 6896–6901, (Pacific Grove, CA).

549 Pednekar, D. D., Amin, M. R., Azgomi, H. F., Aschbacher, K., Crofford, L. J., and Faghah, R. T. (2020).
550 Characterization of cortisol dysregulation in fibromyalgia and chronic fatigue syndromes: a state-space
551 approach. *IEEE Transactions on Biomedical Engineering* 67, 3163–3172

552 Pivonello, R., De Leo, M., Cozzolino, A., and Colao, A. (2015). The treatment of cushing's disease.
553 *Endocrine reviews* 36, 385–486

554 Prerau, M. J., Smith, A. C., Eden, U. T., Kubota, Y., Yanike, M., Suzuki, W., et al. (2009). Characterizing
555 learning by simultaneous analysis of continuous and binary measures of performance. *Journal of
556 neurophysiology* 102, 3060–3072

557 Rinehart, J., Alexander, B., Le Manach, Y., Hofer, C. K., Tavernier, B., Kain, Z. N., et al. (2011). Evaluation
558 of a novel closed-loop fluid-administration system based on dynamic predictors of fluid responsiveness:
559 an in silico simulation study. *Critical Care* 15, 1–12

560 Smith, A. C., Frank, L. M., Wirth, S., Yanike, M., Hu, D., Kubota, Y., et al. (2004). Dynamic analysis of
561 learning in behavioral experiments. *Journal of Neuroscience* 24, 447–461

562 Smyth, N., Rossi, E., and Wood, C. (2020). Effectiveness of stress-relieving strategies in regulating patterns
563 of cortisol secretion and promoting brain health. *International review of neurobiology* 150, 219–246

564 Stalder, T., Kirschbaum, C., Kudielka, B. M., Adam, E. K., Pruessner, J. C., Wüst, S., et al. (2016).
565 Assessment of the cortisol awakening response: expert consensus guidelines. *Psychoneuroendocrinology*
566 63, 414–432

567 Taghvafard, H., Cao, M., Kawano, Y., and Faghah, R. T. (2019). Design of intermittent control for cortisol
568 secretion under time-varying demand and holding cost constraints. *IEEE Transactions on Biomedical
569 Engineering* 67, 556–564

570 Tritos, N. A. and Biller, B. M. (2017). Medical therapies in cushing's syndrome. In *The Hypothalamic-
571 Pituitary-Adrenal Axis in Health and Disease* (Springer). 165–179

572 Van den Berg, G., Frölich, M., Veldhuis, J. D., and Roelfsema, F. (1995). Combined amplification of the
573 pulsatile and basal modes of adrenocorticotropin and cortisol secretion in patients with cushing's disease:
574 evidence for decreased responsiveness of the adrenal glands. *The Journal of Clinical Endocrinology &
575 Metabolism* 80, 3750–3757

576 Vance, M. (2017). Physical presentation of cushing's syndrome: Typical and atypical presentations. In
577 *Cushing's Disease* (Elsevier). 57–65. doi:<https://doi.org/10.1016/B978-0-12-804340-0.00003-6>

578 Venugopal, M., Arya, S. K., Chornokur, G., and Bhansali, S. (2011). A realtime and continuous assessment
579 of cortisol in isf using electrochemical impedance spectroscopy. *Sensors and Actuators A: Physical* 172,
580 154–160

581 Wickramasuriya, D. S. and Faghah, R. T. (2019a). A bayesian filtering approach for tracking arousal from
582 binary and continuous skin conductance features. *IEEE Transactions on Biomedical Engineering* 67,
583 1749–1760

584 Wickramasuriya, D. S. and Faghah, R. T. (2019b). A cortisol-based energy decoder for investigation of
585 fatigue in hypercortisolism. In *2019 41st Annual International Conference of the IEEE Engineering in
586 Medicine and Biology Society (EMBC)* (IEEE), 11–14, (Berlin).

587 Wickramasuriya, D. S. and Faghah, R. T. (2020a). A marked point process filtering approach for tracking
588 sympathetic arousal from skin conductance. *IEEE Access* 8, 68499–68513

589 Wickramasuriya, D. S. and Faghah, R. T. (2020b). A mixed filter algorithm for sympathetic arousal
590 tracking from skin conductance and heart rate measurements in pavlovian fear conditioning. *Plos one*
591 15, e0231659

592 Yang, Y. and Shanelchi, M. M. (2016). An adaptive and generalizable closed-loop system for control of
593 medically induced coma and other states of anesthesia. *Journal of neural engineering* 13, 066019

594 Yu, X., He, W., Li, H., and Sun, J. (2020). Adaptive fuzzy full-state and output-feedback control for
595 uncertain robots with output constraint. *IEEE Transactions on Systems, Man, and Cybernetics: Systems*
596 52, 1–14

597 Zisapel, N., Tarrasch, R., and Laudon, M. (2005). The relationship between melatonin and cortisol rhythms:
598 clinical implications of melatonin therapy. *Drug development research* 65, 119–125

599 Zoukit, A., El Ferouali, H., Salhi, I., Doubabi, S., and Abdennouri, N. (2019). Design of mamdani type
600 fuzzy controller for a hybrid solar-electric dryer: case study of clay drying. In *2019 6th International
601 Conference on Control, Decision and Information Technologies (CoDIT)* (IEEE), 1332–1337, (Paris).

602 Zulfikar, W., Prasetyo, P., Ramdhani, M., et al. (2018). Implementation of mamdani fuzzy method in
603 employee promotion system. In *IOP Conference Series: Materials Science and Engineering* (IOP
604 Publishing), vol. 288, 012147

FIGURES AND TABLES

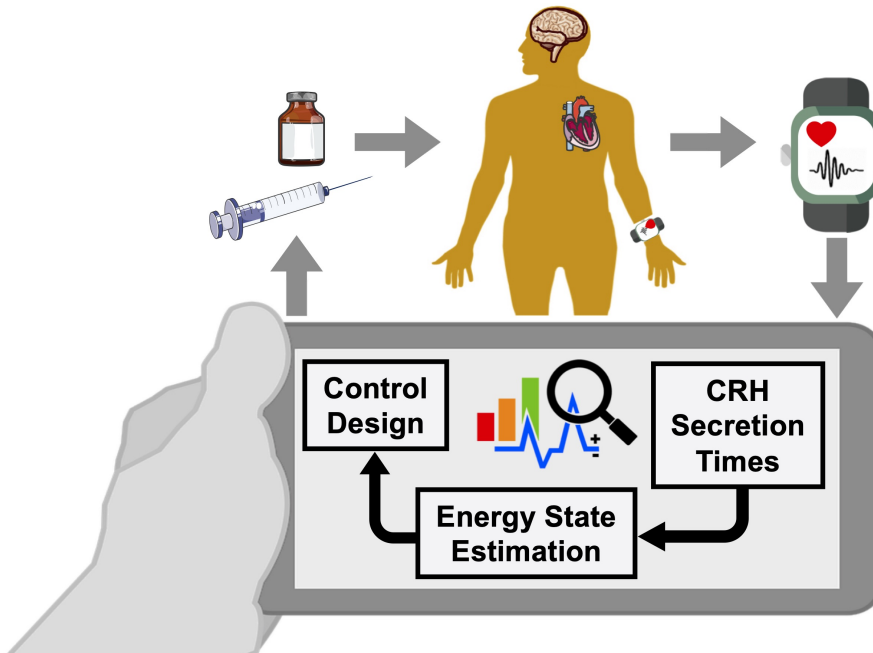


Figure 1. Wearable brain machine interface architecture. Blood cortisol data is being monitored by a wearable-type device. Analyzing the data collected from the human in the loop, we estimate corticotrophin-releasing hormone (CRH) secretion times that result in cortisol secretion. Then, we estimate a hidden energy state. Finally, the designed control algorithm would determine appropriate time and the dosage of medications, and will result in regulating the energy state in patients with hypercortisolism.

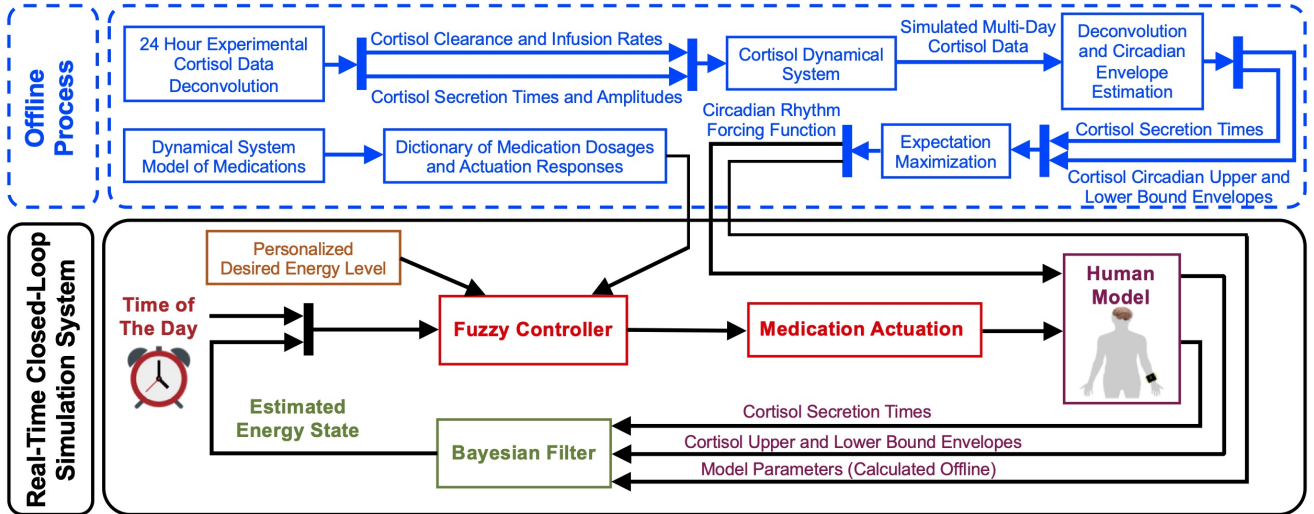


Figure 2. Real-time closed-loop energy regulation. The offline process includes extending the cortisol data profiles for multi-day data creation, simulating the medication dynamics, and estimating the filter parameters required for the closed-loop section. In the real-time closed-loop system, using the state-space representation, the internal energy state gets related to the brain secretion times that result in the cortisol secretions. Then, a Bayesian decoder employs the brain secretion times and the upper and lower cortisol envelopes as the observations to estimate the energy state. Finally, employing the personalized desired energy levels and information regarding the actuation dynamics, a fuzzy controller is generated. The closed-loop system automates the time and dosage of applying simulated medications to regulate the energy state.

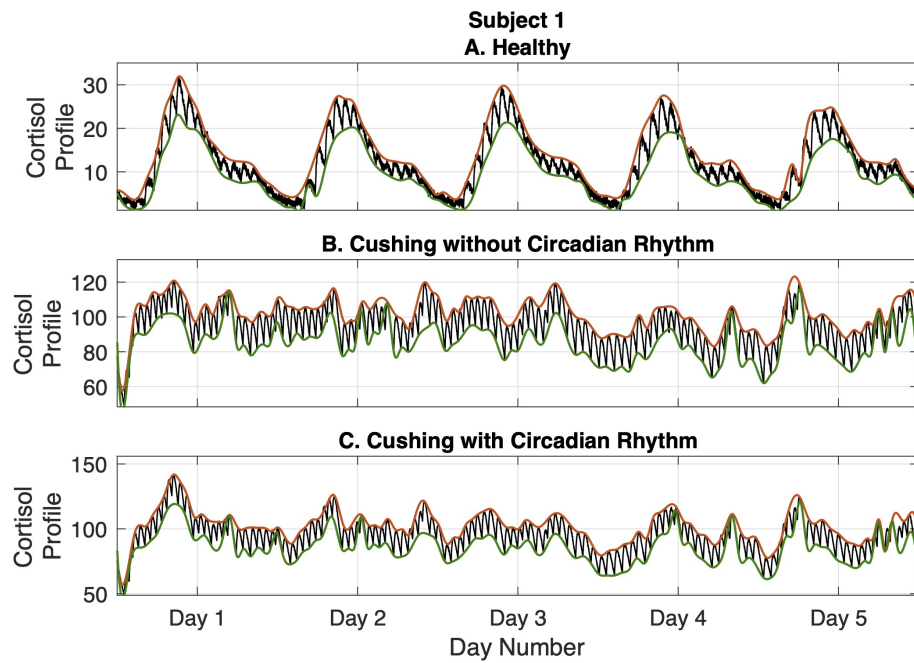


Figure 3. Simulated multi-day cortisol profile - Subject 1. Panel (A) displays the healthy profile, panel (B) shows the profile associated with the Cushing's patients without circadian rhythm, and panel (C) depicts the profiles associated with the Cushing's patients with circadian rhythm. Each panel displays cortisol levels (black curve), upper bound envelopes (orange curve), and lower bound envelopes (green curve).

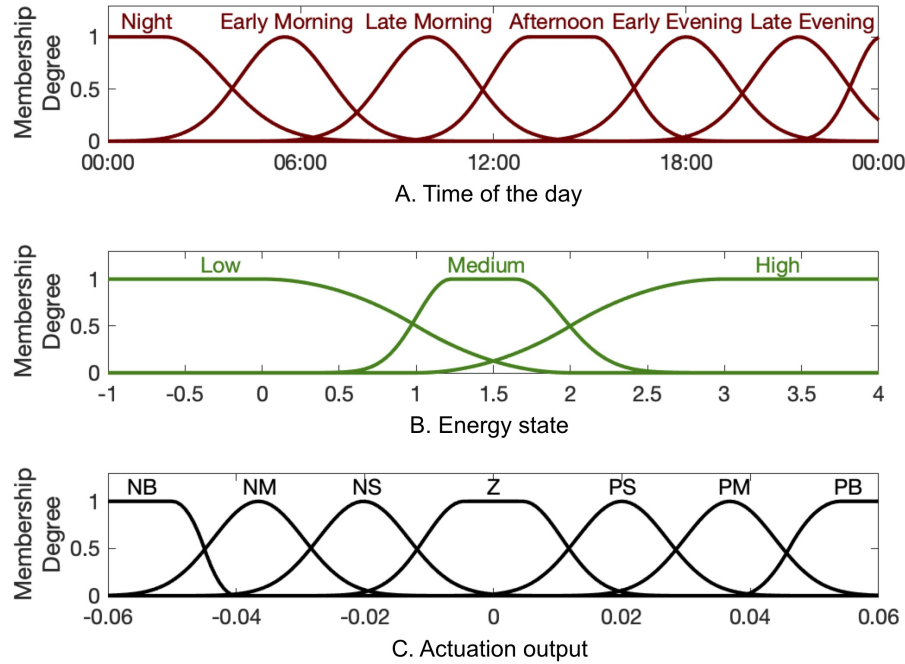


Figure 4. Input and output membership functions. Panel (A) shows the first input membership functions describing time of the day. Panel (B) shows the input membership functions associated with the estimated energy-related state. Panel (C) shows the membership functions for the actuation output (i.e. control signal u_k). The abbreviations P, N, Z, S, M, and B stand for “Positive,” “Negative,” “Zero,” “Small,” “Medium,” and “Big”, respectively.

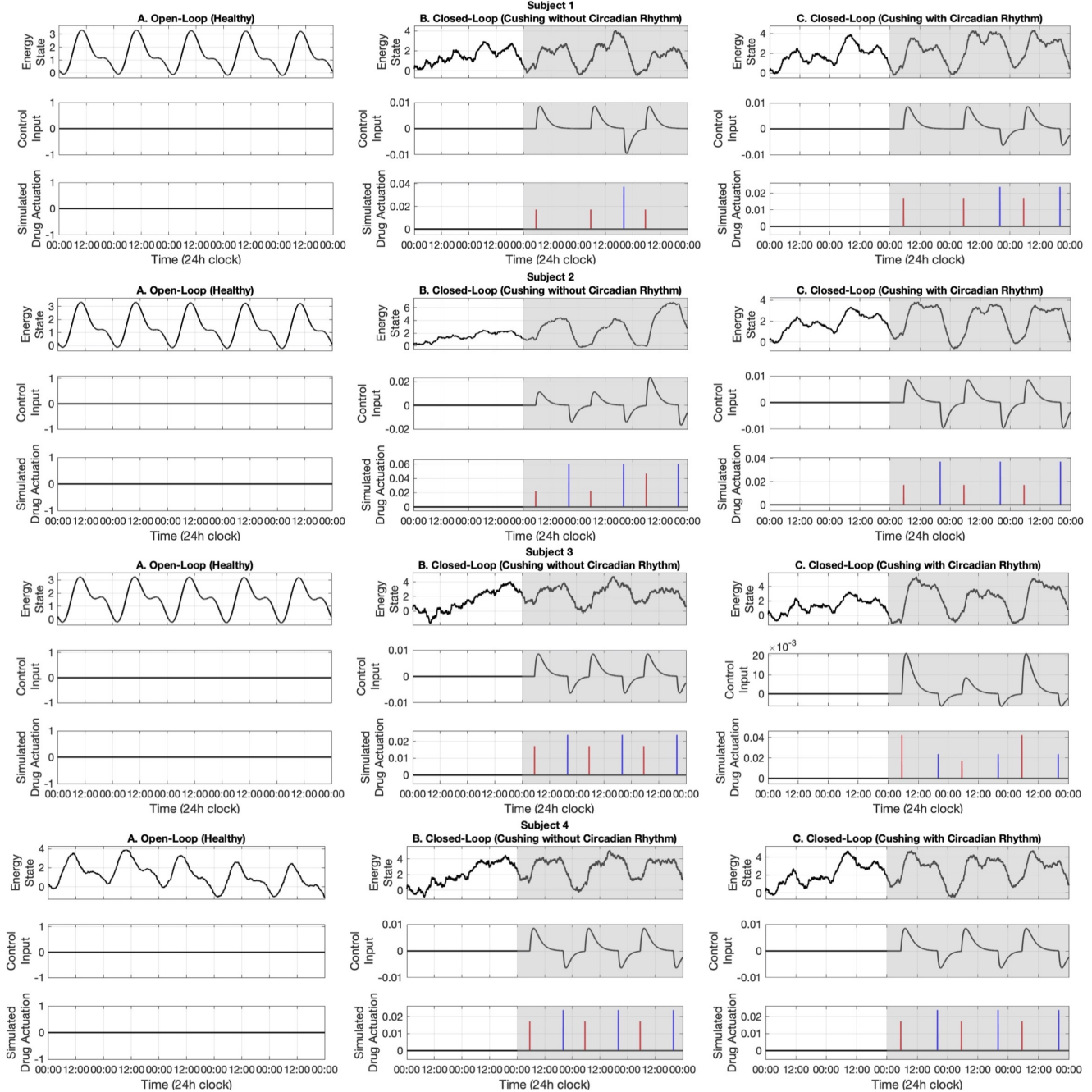


Figure 5. Simulated energy regulation results (Subjects 1-4). For each subject, panel (A) displays the open-loop results. Panel (B) shows closed-loop results for the Cushing's patients without circadian rhythm, while panel (C) shows closed-loop results for the Cushing's patients with circadian rhythm. In each panel: the top sub-panel shows the estimated cognitive energy-related state, the middle sub-panel displays the control input, and the bottom sub-panel depicts the medication injections. Red pulses are related to excitation and the blue pulses are related to inhibition. The white background indicates open-loop simulation (i.e. $u = 0$), while the grey background depicts the closed-loop results.

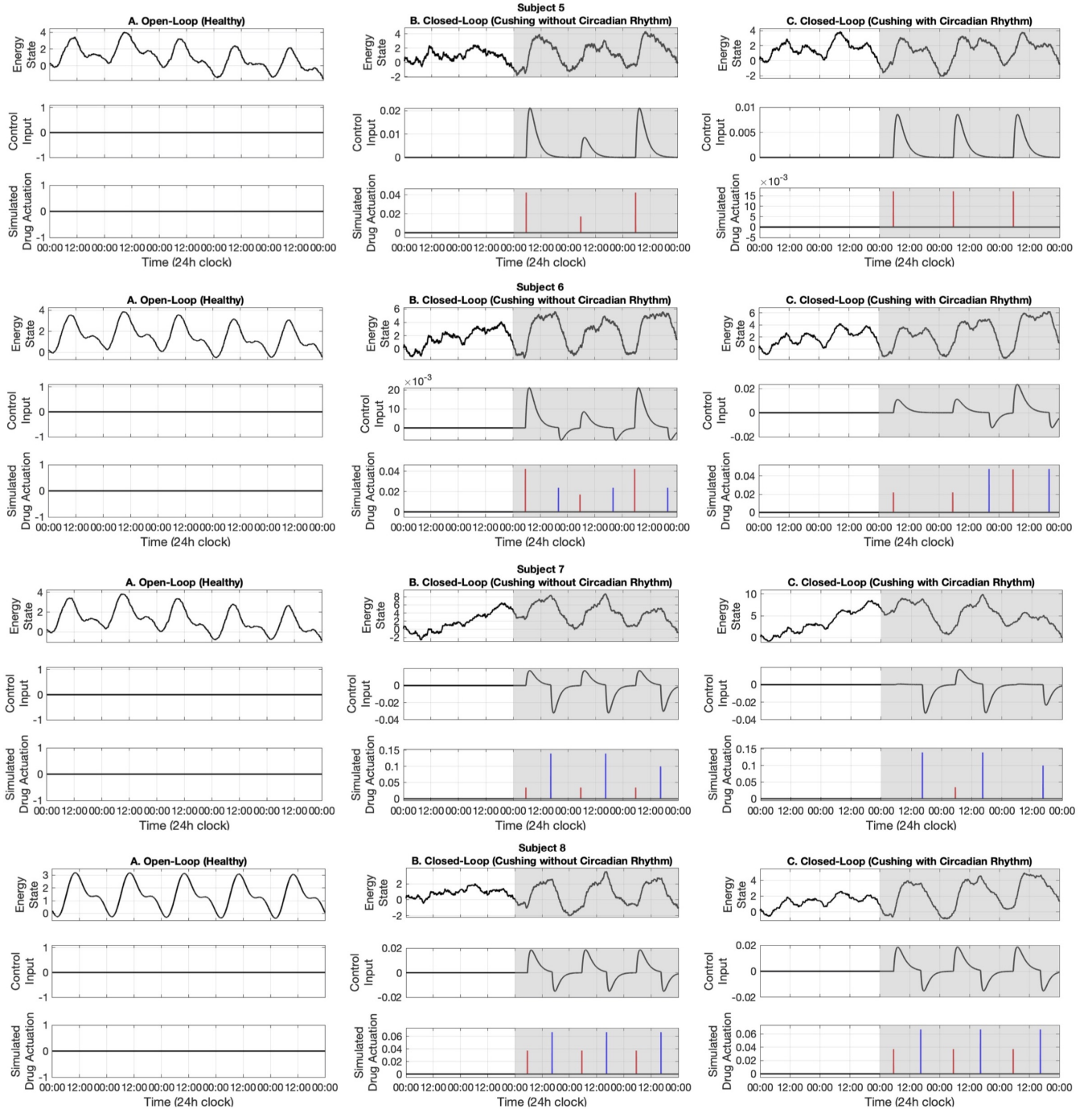


Figure 6. Simulated energy regulation results (Subjects 5-8). For each subject, panel (A) displays the open-loop results. Panel (B) shows closed-loop results for the Cushing's patients without circadian rhythm, while panel (C) shows closed-loop results for the Cushing's patients with circadian rhythm. In each panel: the top sub-panel shows the estimated cognitive energy-related state, the middle sub-panel displays the control input, and the bottom sub-panel depicts the medication injections. Red pulses are related to excitation and the blue pulses are related to inhibition. The white background indicates open-loop simulation (i.e. $u = 0$), while the grey background depicts the closed-loop results.

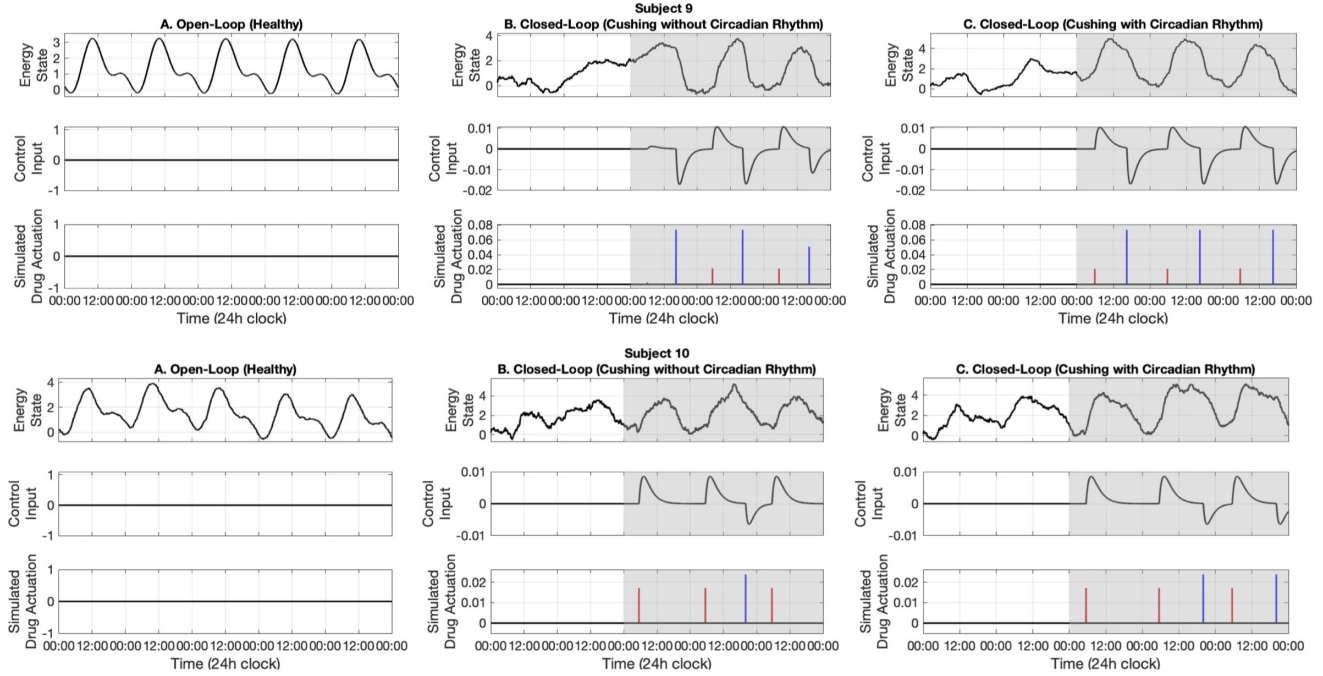


Figure 7. Simulated energy regulation results (Subjects 9 and 10). For each subject, panel (A) displays the open-loop results. Panel (B) shows closed-loop results for the Cushing's patients without circadian rhythm, while panel (C) shows closed-loop results for the Cushing's patients with circadian rhythm. In each panel: the top sub-panel shows the estimated cognitive energy-related state, the middle sub-panel displays the control input, and the bottom sub-panel depicts the medication injections. Red pulses are related to excitation and the blue pulses are related to inhibition. The white background indicates open-loop simulation (i.e. $u = 0$), while the grey background depicts the closed-loop results.

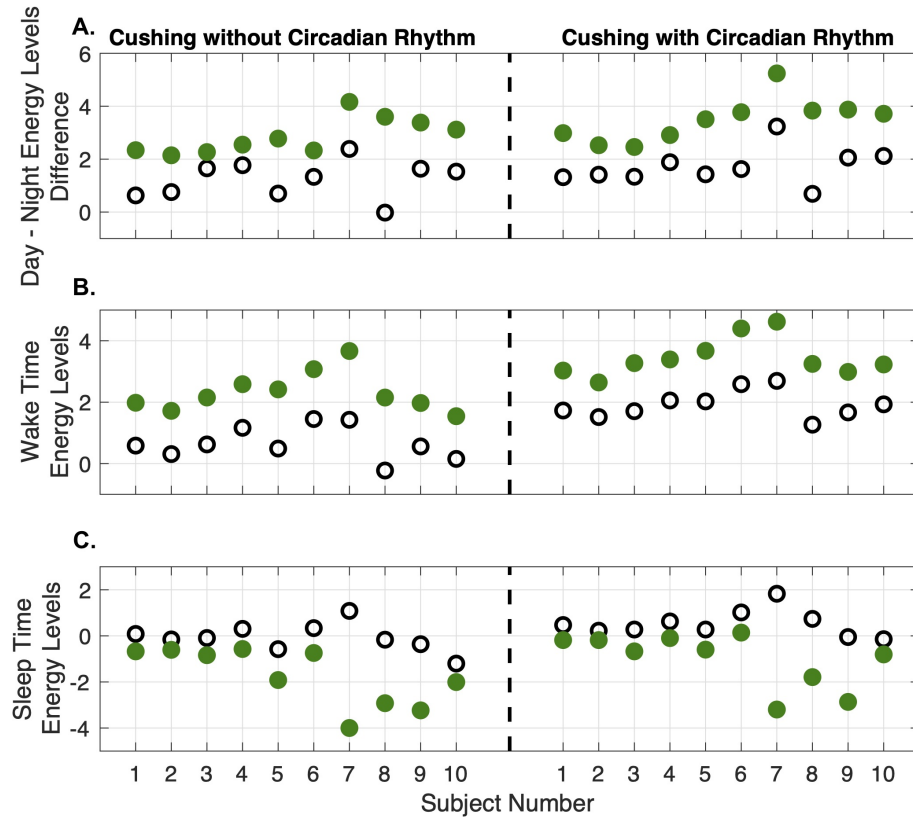


Figure 8. Results analysis. Panel (A) shows the difference between average levels of energy in the day and night. Panel (B) shows the internal energy growth required for the wake-up time balance. Panel (C) shows the decrease in internal energy levels required for sleep time balance. The empty circles and the filled green circles show the results of the open-loop and closed-loop cases, respectively. The left and right sub-panels show the data corresponding to the Cushing patients without and with circadian rhythm in their cortisol profiles, respectively.

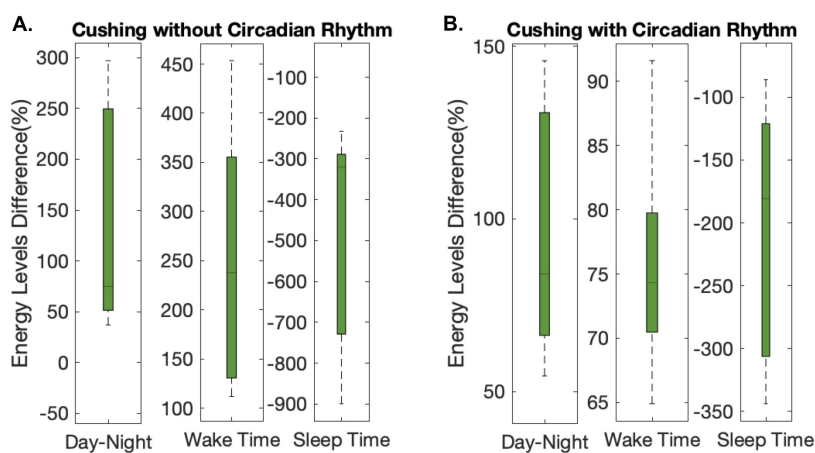


Figure 9. Overall results analysis. The lower- and upper-bounds of the of each box represents the 25th and 75th percentiles of the distribution of each metric for all 10 subjects, and the middle line in each box displays the median. Panels (A) and (B) show the data corresponding to the Cushing patients without and with circadian rhythm in their cortisol profiles, respectively.

Table 1. Fuzzy Rule Base.

| Rule # | Time (<i>Input 1</i>) | Energy State (<i>Input 2</i>) | Actuation (<i>Output</i>) |
|--------|-------------------------|---------------------------------|-----------------------------|
| 1 | Early Morning | High | Positive Small |
| 2 | Early Morning | Low | Positive Big |
| 3 | Early Morning | Medium | Positive Medium |
| 4 | Late Morning | High | Zero |
| 5 | Late Morning | Low | Positive Medium |
| 6 | Late Morning | Medium | Positive Small |
| 7 | Early Evening | High | Negative Medium |
| 8 | Early Evening | Low | Zero |
| 9 | Early Evening | Medium | Negative Small |
| 10 | Late Evening | High | Negative Big |
| 11 | Late Evening | Low | Negative Small |
| 12 | Late Evening | Medium | Negative Medium |